

An impact of a localization of an oxide aperture within a vertical-cavity surface-emitting diode laser (VCSEL) cavity on its lasing threshold

ROBERT P. SARZAŁA

Laboratory of Computer Physics, Institute of Physics, Technical University of Łódź,
ul. Wólczajska 219, 93-005 Łódź, Poland; e-mail: rpsarzal@p.lodz.pl

In the present paper, an impact of localization of an oxide aperture within a vertical-cavity surface-emitting diode laser (VCSEL) on its threshold operation is analyzed. As expected, a shift of the aperture from the anti-node position of the standing optical wave within a VCSEL cavity to the node position is followed by a drastic change of the wave guiding mechanism from the index guiding to the gain guiding. Index-guided VCSELs have been found to exhibit much lower threshold currents, but any increase in their active-region diameters over a relatively low critical value is followed by excitation of higher-order modes. On the other hand, the fundamental-mode operation is achieved in gain-guided VCSELs with much larger active regions but at the expense of considerably higher lasing thresholds. Therefore, a new VCSEL design, *i.e.*, the separate confinement oxidation (SCO) VCSEL, is proposed. The SCO VCSELs are expected to combine advantages of both previous oxide-confined VCSELs, *i.e.*, low lasing thresholds of index-guided VCSELs with the fundamental-mode operation of gain-guided ones even in the case of large active regions.

Keywords: semiconductor laser, vertical-cavity surface-emitting diode laser (VCSEL), oxide-confined VCSELs, fundamental-mode operation.

1. Introduction

A semiconductor diode laser may be understood in the simplest way as a specially designed p - n junction. In its forward-bias condition, electrons and holes are injected into a device active region, where they recombine giving generation of radiation. One of the most fundamental diode-laser parameters, the threshold current for the lasing operation, depends on the active-region volume. In first homojunction diode lasers, carriers could not be effectively confined. Therefore, occupation inversion necessary for lasing requires in these devices extremely high operation currents. This was followed by enormous temperature increases which limited their lasing operation to very low temperatures.

First room-temperature continuous-wave operating diode lasers were demonstrated by HAYASHI *et al.* [1] in 1970. It was possible, in the new heterostructure diode lasers, to enable an efficient carrier confinement in relatively small active regions. Further reduction of their thicknesses below some critical volume was surprisingly found to be followed by a threshold increase. This was connected with an insufficient confinement of the electromagnetic field.

Further structure improvement required an essential structure modification. The new diode-laser structure, *i.e.*, the separate-confinement-heterostructure (SCH), enabled separate confinements of carriers in relatively thin active regions and a radiation field requiring thicker optical cavities. Both confinements are achieved separately, internal heterojunctions are used to confine carriers whereas external ones do not allow radiation out-spreading. Currently most of the diode lasers are equipped with the SCH structures.

Mode selectivity in vertical-cavity surface-emitting diode lasers (VCSELs) depends to a considerable degree on the uniformity of current injection into their active regions. In modern intra-cavity contacted VCSEL structures, this uniformity depends on a radial current flow from annular contacts towards centrally located active regions. Arsenide technology offers the possibility of creating oxide apertures with the aid of radial wet oxidation of Al-rich AlGaAs layers. Then its unaffected central part exhibits much lower electrical resistivity than that of the oxide, which is used to funnel current flow towards the active region. Additionally, refractive index is essentially lower within the oxide (about 1.6 [2]) than in the semiconductor (for GaAs $n_R(1.3 \mu\text{m}) \approx 3.4$). Therefore, oxide apertures may be used not only to radially confine current spreading (electrical apertures) but also to create radial waveguiding effect (optical ones).

Generally, waveguiding mechanism in diode lasers may be associated with distributions of an index of refraction (index guiding) or optical gain (gain guiding).

T a b l e 1. Composition and thickness of structure layers of the 3λ -cavity VCSEL. Some values of model parameters are also given.

Layer	Thickness [nm]	Refractive index n_R	dn_R/dT [10^{-4}K^{-1}]
GaAs upper DBR	28×95.6	3.4	3.0
Al _{0.8} Ga _{0.2} As upper DBR	28×108	3.01	1.47
<i>p</i> -GaAs	360.9	3.4	3.0
Al _{<i>x</i>} O _{<i>y</i>}	50	1.61	0
<i>p</i> -GaAs	341.2	3.4	3.0
Ga _{0.66} In _{0.34} N _{0.017} As _{0.983} QW	2×6.5	3.8	3.0
GaAs barrier	25	3.4	3.0
<i>n</i> -GaAs	260.5	3.4	3.0
Al _{<i>x</i>} O _{<i>y</i>}	15	1.61	0
<i>n</i> -GaAs	89.2	3.4	3.0
GaAs bottom DBR	34×95.6	3.4	3.0
AlAs bottom DBR	34×111.5	2.915	1.34

While manufacturing gain-guided VCSELs is relatively simple and they operate usually on a single fundamental transverse mode, they exhibit relatively high lasing thresholds which is followed by high active-region temperature increases [3]. Index-guided VCSELs are additionally equipped with a radial waveguiding mechanism reducing optical losses. Their lasing thresholds are considerably lower, but at the expense of an unwanted excitation of higher-order transverse modes.

In a standard oxide-confined VCSEL, its oxide aperture is placed in the anti-node position of the resonator optical standing wave. Then it works as both the optical aperture, introducing strong radial waveguiding mechanism, and the electrical one funneling current flow towards the active region. Based on the idea introduced in the SCH lasers, in the present paper, a new separate confinement oxidation (SCO) VCSEL structure is proposed, where both the above confining mechanisms, optical and electrical ones, are created separately. Performance of such a SCO VCSEL will be analyzed in Sec. 4.

2. Structure

Let us consider a typical structure of the 1.3- μm double-oxide-confined (DOC) GaAs-based quantum-well (QW) (GaIn)(NAs)/GaAs 3λ -cavity VCSEL shown in Fig. 1. The thickness and composition of all its structure layers are listed in Tab. 1, where additionally numerical values of some model parameters are given.

The laser active region is similar (but not identical) to the one reported by Infineon Technologies AG [4–7]. It consists of two 6.5-nm (GaIn)(NAs) QWs (double quantum-well (DQW) structure), each containing about 34–35% indium and 1.5–1.8% nitrogen, separated by a 25-nm GaAs barrier, all intentionally undoped (residual 10^{16} cm^{-3} doping is assumed). The active region is sandwiched by the p - and

Tab. 1, continued.

Group refractive index n_G	Absorption coefficient α [cm^{-1}]	$d\alpha/dT$ [$10^{-3}\text{cm}^{-1}\text{K}^{-1}$]
3.654	1	1.28
3.198	1	1.28
3.654	20	1.28
1.681	20	0
3.654	5	1.28
4.62	0	0
3.654	0	0
3.654	2.5	1.28
1.681	2.5	0
3.654	2.5	1.28
3.654	0.5	1.28
3.056	0.5	1.28

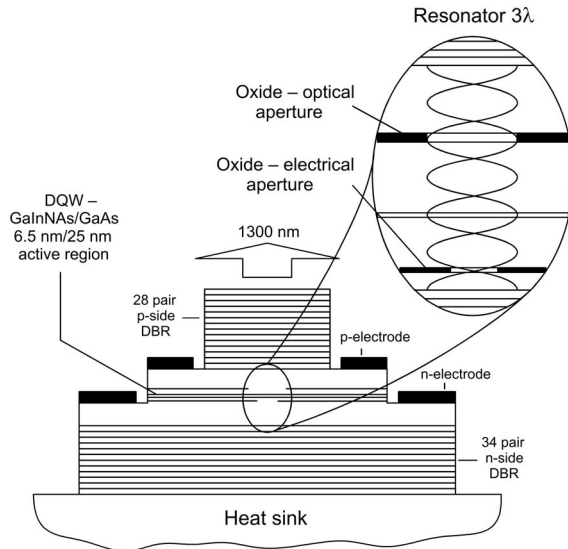


Fig. 1. Structure of the 1.3- μm DOC GaAs-based (GaIn)(NAs)/GaAs QW 3λ -cavity VCSEL.

the n -type GaAs spacers. While the upper part (over the oxide aperture) of the p -type spacer is doped to $2 \times 10^{18} \text{ cm}^{-3}$, the lower one (between the oxide and the active region) is doped to 10^{17} cm^{-3} only. Analogously, the upper part (between the active region and the base of the mesa structure) of the n -type spacer is doped to 10^{16} cm^{-3} only, whereas the bottom one – to 10^{18} cm^{-3} . Relatively high doping of the upper part of the p -type spacer and the bottom part of the n -type one is applied to reduce their electrical resistivities because they are also working as radial-current-spreading layers for a current flow from annular contacts towards the central active region. Unfortunately, higher doping is followed by increasing optical absorption.

The 28 periods of quarter-wave GaAs/ $\text{Al}_{0.8}\text{Ga}_{0.2}\text{As}$ layers (of total reflectivity of 99.9350%) and analogous 34 periods of GaAs/AlAs layers (99.9943%) are assumed correspondingly as upper and bottom distributed-Bragg-reflector (DBR) resonator mirrors. Their diameters are equal to 50 and 100 μm , respectively. Two (n - and p -side) annular contacts are deposited on both GaAs spacer layers (see Fig. 1). Internal contact diameters are postulated to be equal to 54 μm (p -side) and 74 μm (n -side), respectively, whereas external ones – to 70 and 100 μm . Typical values of their contact resistances are equal to $10^{-5} \Omega\text{cm}^2$ (n -side) and $10^{-4} \Omega\text{cm}^2$ (p -side).

3. Model

The simulation model is composed of four interrelated parts. The optical one is based on the effective-frequency method. Current-density profiles are determined from potential distributions found using the Laplace equation and the concept of the effective active-region conductivity. Temperature profiles are calculated assuming the

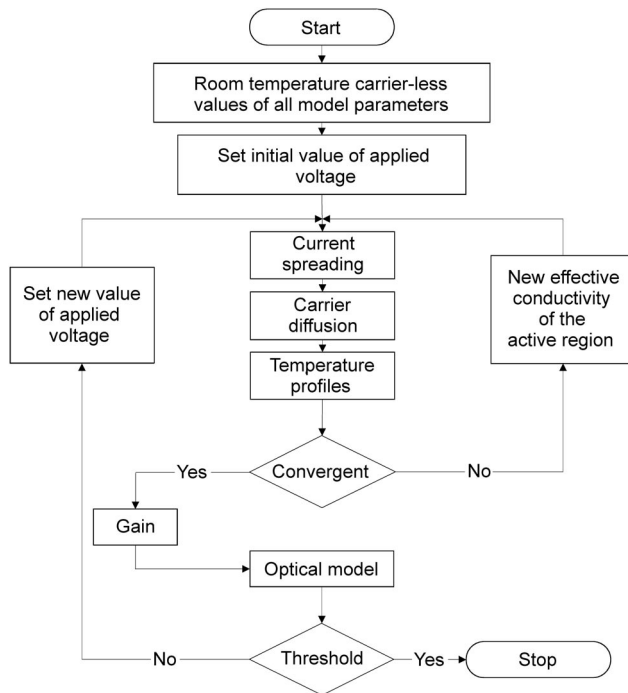


Fig. 2. Self-consistent calculation algorithm.

active region heating (non-radiative recombination and absorption of the spontaneous radiation) and volume and barrier Joule heating as well as a dominant heat-abstraction mechanism through the device heat sink. The classical Fermi's golden rule, the parabolic band-gap approximation and the Lorentzian broadening mechanism are used to determine QW gain spectra. The model is developed taking into consideration principles given by [8]. Its more detailed description was reported earlier [9, 10] and its schematic flow chart is given in Fig. 2.

4. Results

An impact of a localization of single or double oxidation apertures within the VCSEL cavity on a device threshold operation has been analyzed. In VCSELs with a single oxide aperture of the diameter $2r_A$, it is assumed to be located not only in the anti-node position of the optical standing wave (the SA structure), where it works as both the optical and electrical aperture, but also in all other locations including the analogous node position (the SN structure), where there are only the electrical apertures. When two oxide apertures are considered, one of them is assumed to be placed in the anti-node position, whereas the second one – in the node position. Two cases are analyzed, the D structure with identical both apertures and the new SCO structure with reduced diameters $2r_E$ of the electrical aperture. Thicknesses of all oxide layers are assumed

Table 2. Threshold parameters determined for various room-temperature operating VCSEL structures: SN – VCSEL structure with a single oxide aperture located at the standing-wave node position, SA – analogous VCSEL structure with the aperture shifted to the anti-node position, D – VCSEL with two identical apertures, the first one at the node and the second at the anti-node position, SCO – the proposed new VCSEL structure with two oxide apertures of different diameters: the larger (r_A) optical aperture is placed at the anti-node position whereas the smaller (r_E) electrical one – at node position; U_{th} – threshold voltage, I_{th} – threshold current, $T_{A, max}$ – maximal active-region temperature, $g_{th, max}$ – maximal threshold optical gain, mode – the lowest-threshold transverse mode, λ – wavelength of emitted radiation.

Number and symbol of structure	r_A [μm]	r_E [μm]	U_{th} [V]	I_{th} [mA]	$T_{A, max}$ [K]	$g_{th, max}$ [cm^{-1}]	Mode	λ [nm]
1 SN	10	–	3.65	21.13	316.83	4432	LP ₀₁	1303.2
2 SCO	10	7.5	2.64	9.97	307.77	3128	LP ₀₁	1299.5
3 SN	7.5	–	2.55	10.22	308.16	2792	LP ₀₁	1302.4
4 SCO	7.5	5	1.95	4.60	304.30	2094	LP ₀₁	1300.0
5 SA	7.5	–	1.94	5.72	303.76	1539	LP ₇₁	1295.8
6 SN	5	–	1.99	5.11	305.18	2174	LP ₀₁	1302.1
7 SCO	5	3.75	1.55	2.36	302.59	1518	LP ₀₁	1298.7
8 SA	5	–	1.68	3.22	302.91	1311	LP ₃₁	1297.1
9 SN	2	–	2.75	4.85	315.68	6890	LP ₀₁	1302.3
10 D	2	2	1.20	0.65	301.20	884	LP ₀₁	1296.6
11 SA	2	–	1.27	0.86	301.50	1189	LP ₀₁	1298.2

to be equal to 15 nm, whereas aperture radii have been changed from 2 to 10 μm . Some simulation results are listed in Tab. 2. Temperature and gain profiles are very nonuniform within VCSEL active regions [11] (these nonuniformities drastically increase with an increase in the active-region diameter), therefore only their maximal values close to the active-region edges are given.

In SN VCSELs, in which a single oxide aperture is working as the electrical aperture only, the waveguiding mechanism is associated solely with the optical-gain profile. In such gain-guided VCSELs, a stable single-mode operation on the fundamental LP₀₁ mode has been found for a wide range of oxide apertures (see 1, 3, 6 and 9 lines in Tab. 2). It seems to enable a considerable increase in the single-fundamental-mode output. Unfortunately, with an increase in the active-region diameter, optical gain profiles are becoming more and more nonuniform. Then the gain is practically confined to a narrow ring area close to the active-region edge and its overlapping with the LP₀₁ fundamental mode is drastically reduced. Therefore, as one can see, this stable single-fundamental-mode operation may be reached only at the expense of a considerable increase in the lasing threshold (see line 1 in Tab. 2). When smaller active regions are considered, a considerable part of the LP₀₁ mode profile is penetrating lateral passive areas which again increases lasing threshold (line 9 in Tab. 2). In this case, an increase in the current density is followed not only by the optical gain increase but it creates an additional radial real waveguiding effect, supporting the gain-induced one, because of the temperature dependence of refractive indices.

When a single oxide aperture is located in the antinode position (SA structure), it not only confines the current spreading, as in SN structures, but also creates a very strong real index-guiding mechanism for the radiation field. It drastically reduces optical losses in VCSELs with small active regions which is followed by a considerable decrease in their lasing thresholds: threshold voltage is reduced by a factor of over two and threshold current – by a factor of over five (*cf.* lines 9 and 11). Besides, the temperature increase is reduced ten times.

The above effect is distinctly smaller in VCSELs with larger active regions. For oxide aperture diameters equal to 10 μm , lasing thresholds are much less sensitive to their locations (*cf.* lines 6 and 8). However, also in this case, a strong real index guiding and a very nonuniform active-region gain profile within the SA structure are followed by an unprofitable excitation of higher-order transverse modes (line 8), whereas the SN structure still exhibits a stable single-fundamental-mode operation (line 6).

An essential improvement in performance of oxide-confined VCSELs may be achieved with the aid of the second oxide aperture. The first one of diameter $2r_A$ is assumed to be located at the anti-node position of the optical standing wave within the VCSEL cavity, whereas the second one, of diameter $2r_E$, is shifted to the analogous node position (see insert of Fig. 1). This enables independent creation of both the radial index-guiding and the active-region gain profile because the second aperture practically does not influence the optical field. Then its diameter may be reduced improving the current confinement in the central part of the active region. To some extent, this structure is a radial equivalent of the SCH created in the direction perpendicular to layer boundaries. By analogy, the new VCSEL structure with an independent creation of the active-region current-density profile and of the radial index-guiding is called the SCO structure. Its advantages have been confirmed by computer simulations.

Figure 3 presents comparison of radial current-density profiles $j_{\text{th}}(r)$ determined for the VCSEL with two identical ($r_A = r_E$) small (5 μm) or large (10 μm) diameters of oxide apertures (D structure) with the same profile found for the new SCO structure. The radius r_E of the electrical aperture has been optimized to minimize the threshold current. As one can see, uniformity of current injection into the active region has been considerably improved in the SCO structure becoming comparable with that of the smaller D VCSEL while, from the optical point of view, its active region is large, similarly to large D VCSEL.

New SCO VCSELs (lines 2, 4 and 7 in Tab. 2) demonstrate threshold currents and active-region temperature increases reduced by a factor of more than two as compared with SN VCSELs with a single oxide aperture located at the standing-wave node position (lines 1, 3 and 6). In all cases, a stable single-fundamental-mode operation has been found. This may be explained by curves shown in Fig. 4 presenting radial intensity profiles found for lasing thresholds in VCSELs of the same active region diameter of 15 μm and three structures considered in this paper: the SA, SN and SCO ones. For the SA structure with the oxide aperture located at the anti-node standing-wave position, a very nonuniform profile of the current injection together

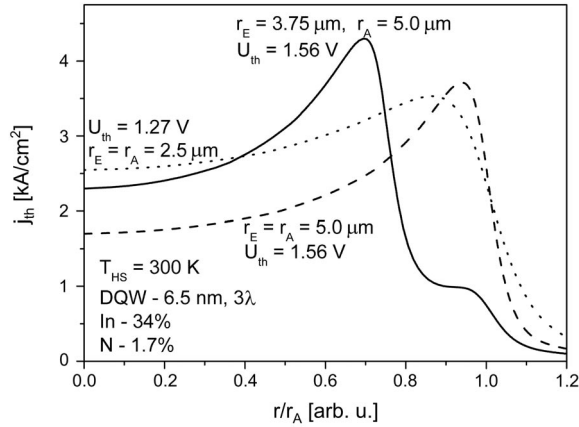


Fig. 3. Radial threshold current density j_{th} profiles of VCSEL devices with both identical oxide apertures (large – dashed line and small – dotted line) and for the proposed large VCSEL device with different apertures (solid line).

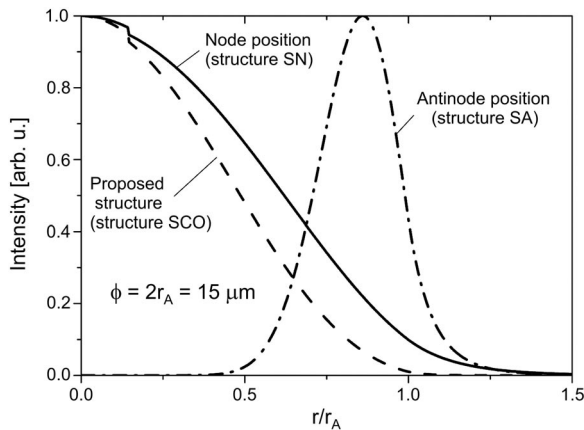


Fig. 4. Radial intensity profiles of the lowest-threshold transverse modes determined for three VCSEL structures considered in the text.

with strong radial index guiding enhance excitation of unwanted higher-order transverse modes of which maxima are close to the active-region edge. The order of the lowest-threshold transverse modes increases with the active-region diameter (*cf.* lines 11, 8 and 5). When the oxide aperture is shifted to the node position (SN structure), the strong index guiding disappears and the radiation field is confined by a much weaker gain guiding. Then the fundamental LP_{01} mode is excited even in the case of large active regions, but too weak radial waveguiding (see Fig. 4) is followed by a considerable threshold increase (*cf.* lines 5 and 3). The proposed SCO structure effectively confines the radiation field within the central part of its active region. At the same time its much better current-density confining enables better overlapping of

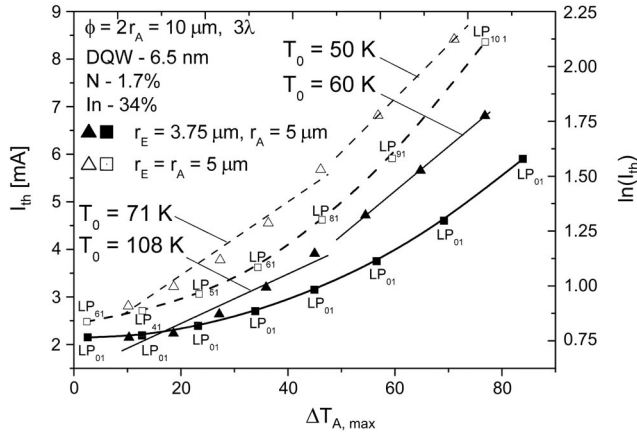


Fig. 5. Threshold currents I_{th} determined for active regions detuned at RT and for large ($\phi = 2r_A = 2r_E = 10 \mu\text{m}$) D-type VCSEL devices with both identical oxide apertures (dashed lines) and for new SCO-type VCSELs with different apertures ($\phi = 2r_A = 10 \mu\text{m}$, $2r_E = 7.5 \mu\text{m}$) vs. an increase in their maximal active-region temperature rise $\Delta T_{A, \text{max}}$. While squares correspond to the left-hand side axis, triangles – to the right-hand one. The lowest-threshold transverse LP modes are indicated. Determined values of the T_0 parameter are given.

the optical gain and the fundamental-mode intensity profiles constraining the single LP_{01} mode excitation.

The new SCO VCSEL has been found to operate on a single fundamental LP_{01} transverse mode for a wide range of active-region temperature increases $\Delta T_{A, \text{max}}$ over room temperature of the ambient (Fig. 5). On the contrary, in the case of the standard D structure with two identical apertures, an increase in the active-region temperature is followed by a rapid increase in the lowest-threshold mode order. Apart from that, threshold current increases with temperature much slower in the SCO VCSEL and its T_0 parameter is as high as 108 K for $\Delta T_{A, \text{max}}$ up to 45 K, and is reduced to still high 60 K for higher temperature increases.

5. Conclusions

The new SCO VCSEL structure demonstrates advantages of both the previous oxide-confined VCSELs: stable single-fundamental-mode operation of the gain-guided VCSEL with the oxide aperture located at the standing-wave node position and a relatively low lasing threshold of the index-guided VCSEL with the aperture shifted to the analogous anti-node position. Besides, observed in SCO VCSELs reduction of both the threshold current and the active-region temperature increase is followed by lower threshold gain values which is very important in new VCSEL structures with $\text{In}(\text{Ga})\text{As}/\text{GaAs}$ quantum-dot or $\text{GaInNAs}(\text{Sb})$ quantum-well active regions.

Summing up, the traditional VCSEL design with the oxide aperture located at the standing-wave node position may be recommended for room-temperature operation

(because of its simple technology) for VCSELs with relatively large regions exhibiting high optical gain and manufactured using a well known technology. In all other cases, the new SCO VCSEL structure ensures much better performance.

Acknowledgements – The work was supported by the Polish State Committee for Scientific Research (KBN), grant No 4-T11B-014-25.

References

- [1] HAYASHI I., PANISH M.B., FOY P.W., SUMSKI S., *Junction lasers which operate continuously at room temperature*, Applied Physics Letters **17**(3), 1970, pp. 109–11.
- [2] KITATANI T., KONDOW M., *Characterization of the refractive index of lateral-oxidation-formed Al_xO_y by spectroscopic ellipsometry*, Japanese Journal of Applied Physics, Part 1: Regular Papers, Short Notes and Review Papers **41**(5A), 2002, pp. 2954–7.
- [3] TOMCZYK A., SARZAŁA R.P., CZYSZANOWSKI T., WASIAK M., NAKWASKI W., *Fully self-consistent three-dimensional model of edge-emitting nitride diode lasers*, Opto-Electronics Review **11**(1), 2003, pp. 65–75.
- [4] RIECHERT H., RAMAKRISHNAN A., STEINLE G., *Development of InGaAsN-based 1.3 μ m VCSELs*, Semiconductor Science and Technology **17**(8), 2002, pp. 892–7.
- [5] STEINLE G., RIECHERT H., EGOROV A.YU., *Monolithic VCSEL with InGaAsN active region emitting at 1.28 μ m and CW output power exceeding 500 μ W at room temperature*, Electronics Letters **37**(2), 2001, pp. 93–5.
- [6] STEINLE G., MEDERER F., KICHERER M., MICHALZIK R., KRISTEN G., EGOROV A.YU., RIECHERT H., WOLF H.D., EBELING K.J., *Data transmission up to 10 Gbit/s with 1.3 μ m wavelength InGaAsN VCSELs*, Electronics Letters **37**(10), 2001, pp. 632–4.
- [7] RAMAKRISHNAN A., STEINLE G., SUPPER D., STOLZ W., EBBINGHAUS G., *Nitrogen incorporation in (GaIn)(NAs) for 1.3 μ m VCSEL grown with MOVPE*, Journal of Crystal Growth **248**, 2003, pp. 457–62.
- [8] OSIŃSKI M., NAKWASKI W., [In] *Vertical-Cavity Surface-Emitting Laser Devices*, [Eds.] H. Li, K. Iga, Springer, Berlin 2003.
- [9] SARZAŁA R.P., *Computer simulation of performance characteristics of (GaIn)(NAs) diode lasers*, Optica Applicata **32**(3), 2002, pp. 449–60.
- [10] SARZAŁA R.P., *Modeling of the threshold operation of 1.3- μ m GaAs-based oxide-confined (InGa)As-GaAs quantum-dot vertical-cavity surface-emitting lasers*, IEEE Journal of Quantum Electronics **40**(6), 2004, pp. 629–39.
- [11] SARZAŁA R.P., NAKWASKI W., *Optimization of 1.3 μ m GaAs-based oxide-confined (GaIn)(NAs) vertical-cavity surface-emitting lasers for low-threshold room-temperature operation*, Journal of Physics: Condensed Matter **16**(31), 2004, S3121–40.

Received June 6, 2005